Supplemental Information (SI)

Experimental Model and Subject Details

Animals

All mice strains have been published: *Ai14* Cre-reporter (1), *Lhx6-GFP* (GENSAT) Tg(Lhx6-EGFP)BP221Gsat, *Nf1*^{flox} (2), *Nkx2.1-Cre* (3) and *PV-Cre* (4). *Nf1*^{flox} mice were initially on a mixed C57BL6/J, CD-1 background, then backcrossed to CD-1 for at least four generations before analysis. For timed pregnancies, noon on the day of the vaginal plug was counted as embryonic day 0.5. Both male and female mice were assessed. We did not observe any gross differences between genders and combined all data for each genotype. All animal care and procedures were performed according to the Michigan State University and University of California San Francisco Laboratory Animal Research Center guidelines.

Antibodies

Primary antibodies used: Goat anti-ChAT, 1:100 (Millipore Sigma, AB144P); Chicken anti-GFP, 1:2000 (Aves); Mouse anti-Kv3.1, 1:400 (NeuroMab, clone N16b/8); Mouse anti-LHX6, 1:200 (Santa Cruz A-9, sc-271433); Rabbit anti-NG2, 1:400 (gift from Bill Stallcup); Rabbit anti-OLIG2 1:500 (Millipore Sigma, AB9610); Rabbit anti-parvalbumin, 1:400 (Swant, PV27); anti-PDGFR-alpha, 1:400 (Cell Signaling, 3174); anti-PH3 1:500 (Cell Signaling, 9701; Rat anti-somatostatin, 1:200 (Millipore Sigma, MAB354); Biotinylated Vicia Villosa Lectin (VVA), 1:300 (Vector Labs, B-1235). Alexa fluorophore secondary antibodies were used at 1:300 (Thermo Fisher). Fluorescein Avidin D (Vector Labs) was used to detect biotinylated VVA.

Cell Counting

We prepared either 20 µm thick cryo-sectioned coronal tissues, for embryonic and postnatal day 2 ages, or 25 µm sections for P30 young adult ages. To determine cell density (cells/mm^2), we counted the number of cells in a given section from the neocortex, hippocampus or striatum and then divided by the area of that region. To calculate the % of tdTomato$^+$ cells that co-labeled with specific markers, we divided the number of co-labeled cells by the total number of tdTomato$^+$ cells.

EdU labeling

Pregnant mice with either E13.5 or E15.5 embryos were pulsed with EdU (10mg/ml) at a dose of 50mg Edu/kg body weight as previously described (5). After 30 minutes, mice were sacrificed, and embryos collected in ice-cold PBS (pH 7.2). Embryos were put in 4% PFA and fixed overnight at 4°C and sunk in 30% sucrose before embedding in OCT. Edu$^+$ cells were visualized by following standard procedures in the Clik-iT EdU plus kit (Thermo Fischer) and then co-stained with antibodies before being labeled with DAPI.

Fluorescent in situ hybridization (FISH)

www.pnas.org/cgi/doi/10.1073/pnas.1915458117

FISH was performed according to (6). Brain tissue from *Nkx2.1-Cre*-lineage P30 WT and *Nf1* cKOs were perfused and incubated with 4% PFA for 1 hour, following by 30% sucrose/PBS cryoprotection until the day of section. Tissues were embedded in OCT and cryo-sectioned to generate 40um tissue sections. To generate the *Nf1* DNA vector and riboprobe, *Nf1* cDNA was PCR amplified from a homemade mouse cDNA library synthesized from P0 neocortex using Superscript II. The following primers are used: 5' GAG AAT CGA TCC CTC ACA GCT TCG AAG TGT and 3' ATA TTC TAG AGG ACC CAG ATA CGC GAG AAG. ClaI and XbaI restriction enzymes sites were introduced (underlined). The primers target the *Nf1* floxed region (exons 31 and 32). Next, the *Nf1* PCR product and the vector, pSP73 (Promega Cat # P2221), were digested with ClaI and XbaI, and then ligated. The *Nf1* RNA anti-sense fluorescein-labeled probe was generated by T7 RNA polymerase (Roche) and a Fluorescein labeling kit (Roche) from a NdeI linearized vector; size of the probe was 572bp. Imaging was done with 60X objective (Nikon Apo 1.4 oil) under Nikon Ti micsroscope with DS-Qi2 color camera.

Single CIN *Nf1* RNA transcript assessment

The unique transcripts per million for different CIN groups and subgroups was determined using the previously described dataset (7). Briefly, the unique *Nf1* transcripts per million were assessed from a combination of Cre, Flp and the appropriate reporter mice in CINs from young adult mice. The CIN types probed were chandelier, parvalbumin-lineage, somatostatin-lineage that were either nitric oxide synthase-1 or calretinin expressing as well as vasoactive intestinal peptide-lineages that were either calretinin or cholecystokinin expressing.

Quantification and statistical analysis

For anatomical analyses, statistics were performed using Prism version 6, a p value of < 0.05 was considered significant. For all parametric measurements of three or more groups, we used a One-Way ANOVA with either Bonferroni or Tukey post test to determine significance. For parametric measures of two groups, a two-tailed T-test was performed. For non-parametric data sets, we used a Chi-squared test to determine significance.

Supplemental Figure 1

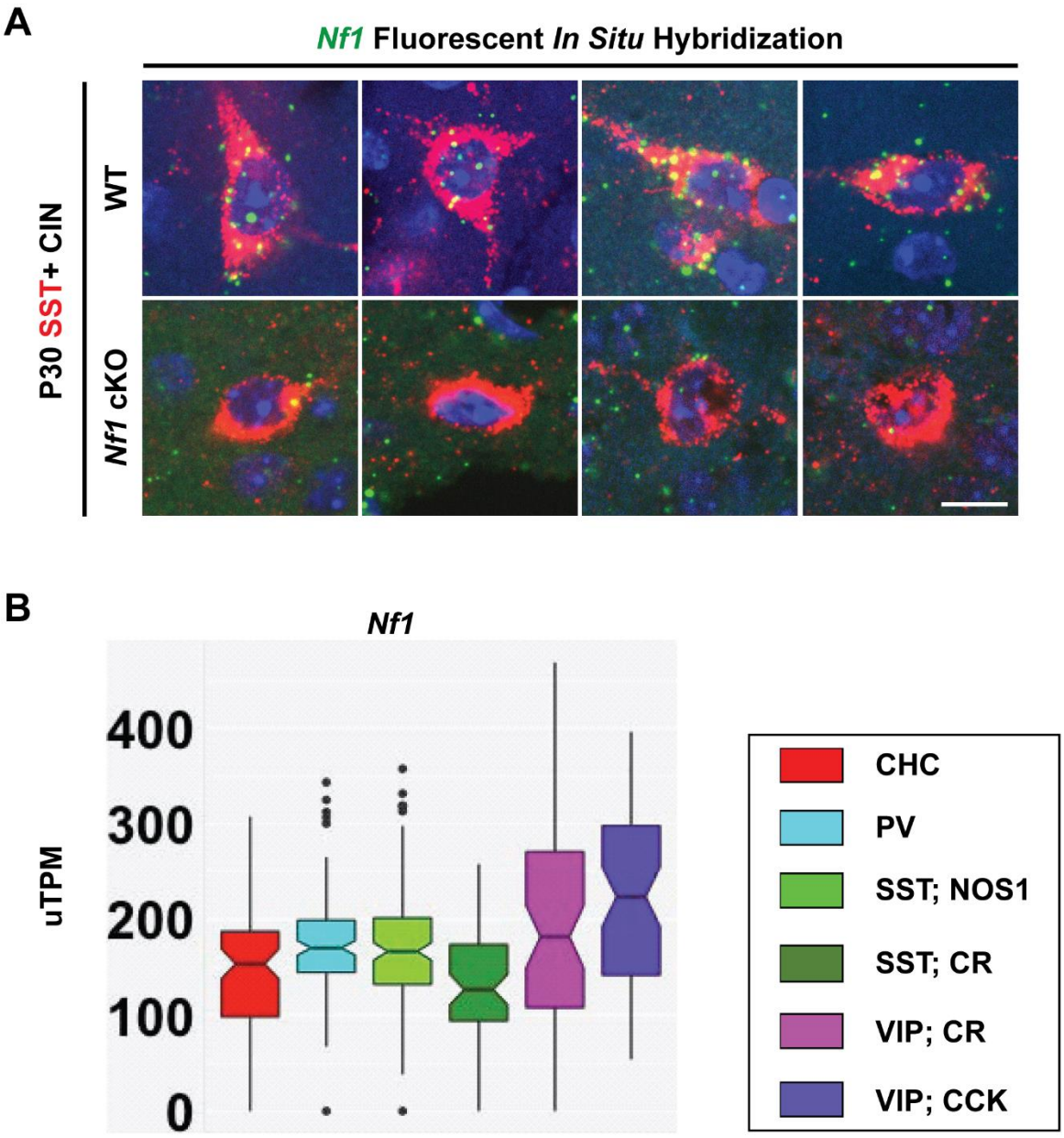

Supplemental Figure 1: *Nf1* transcript is found in most CIN classes and validation of transcript loss in *Nkx2.1-Cre*-lineage SST+ CINs in adult cortex.

(**A**) Fluorescent *in situ* hybridization (FISH) for the floxed *Nf1* exon in P30 WT (top panels) and *Nf1* cKOs (bottom panels) in the somatosensory cortex. *Nf1* transcript was co-stained with SST to verify expression and loss in MGE-derived CINs. *Nf1* transcript levels from purified single CINs from P28-P35 cortex using distinct Cre-driver lines (**B**). Box plots show quantification of the unique transcripts per million (uTPM) from single CIN cells. Single dots represent outlier values. (CHC) chandelier cell, (PV) parvalbumin, (SST) somatostatin (NOS1) nitric oxide synthase, (CR) calretinin, (VIP) vasoactive intestinal peptide, (CCK) cholecystokinin. Scale bar in (**A**) = 20 µm.

Supplemental Figure 2

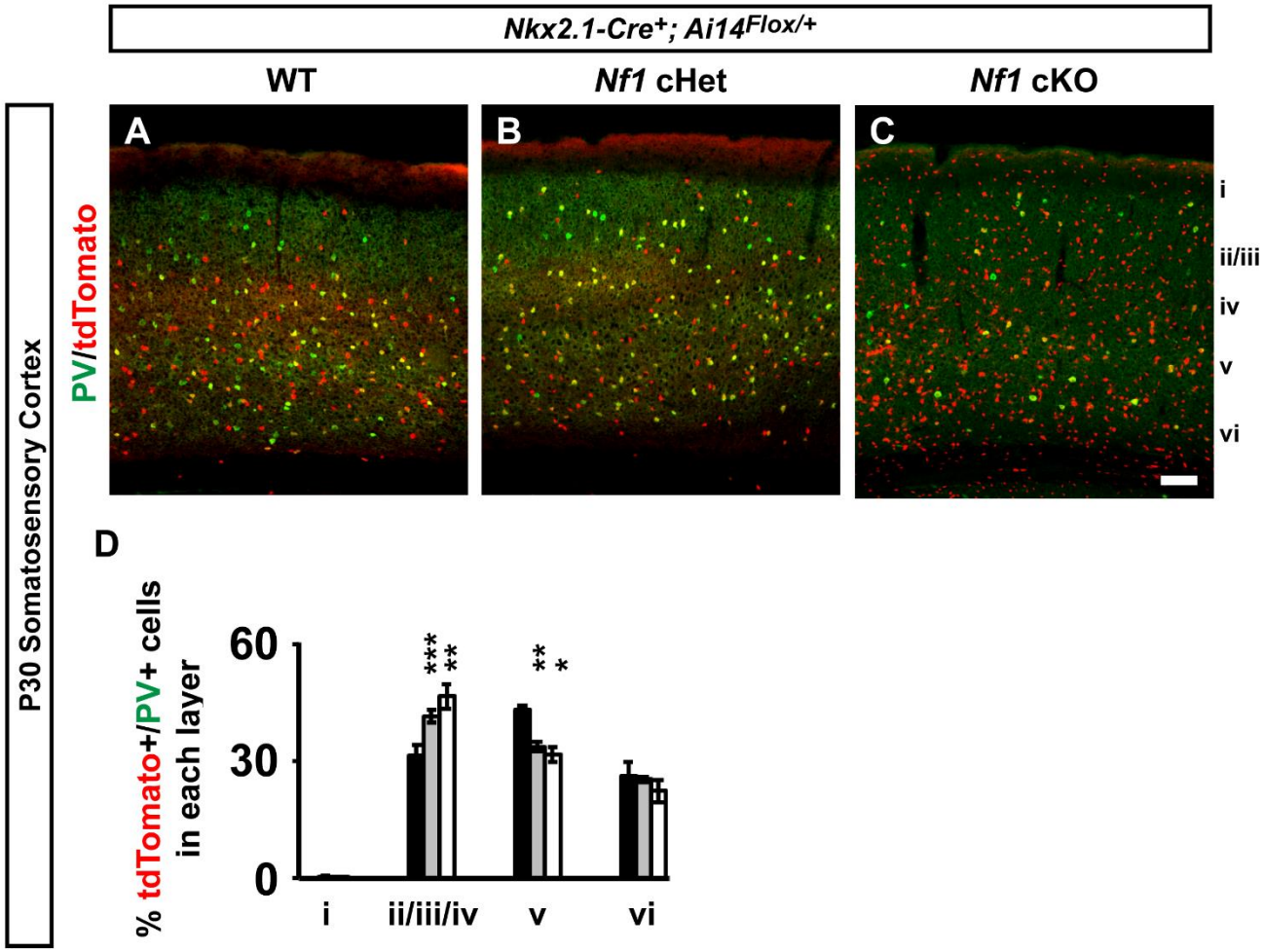

Supplemental Figure 2: Example of merged fluorescent images and laminar counts.

Panels (A-C) show the PV labeled WT, *Nf1* cHet and *Nf1* cKO CINs from Figure 2A-2C merged with tdTomato (*Nkx2.1-Cre*-lineages) in P30 neocortices. (**D**) Quantification of CIN laminar distribution in the neocortices of each genotype at P30. Data are expressed as the mean ± SEM. All groups, n = 4. * $p < 0.05$, ** $p < 0.01$, *** $p < 0.001$. Scale bar in (**C**) = 100 µm.

Supplemental Figure 3

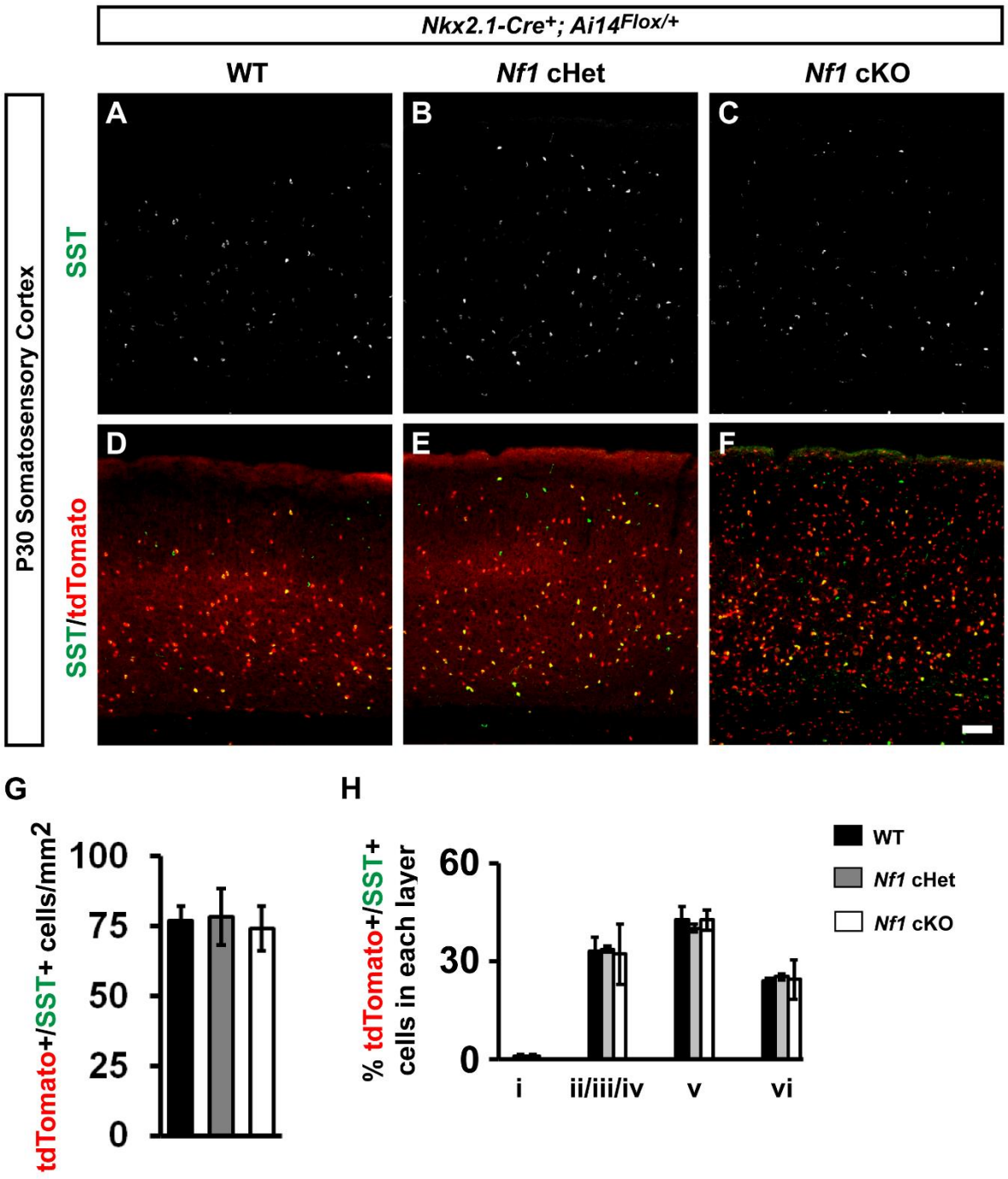

Supplemental Figure 3: No changes in SST+ CINs after loss of *Nf1*.

P30 somatosensory cortices from WTs, cHets and cKOs were labeled for SST (**A-C**) and merged with tdTomato+ *Nkx2.1-Cre* lineages (**D-F**). (**G**) Quantification of the cell density of tdTomato+/SST+ CINs in the somatosensory cortex at P30. (**H**) Quantification of the proportion of tdTomato+/SST+ cells in each cortical lamina. Data are expressed as the mean ± SEM. All groups, n = 4. Scale bar in (**F**) = 100 µm.

Supplemental Figure 4

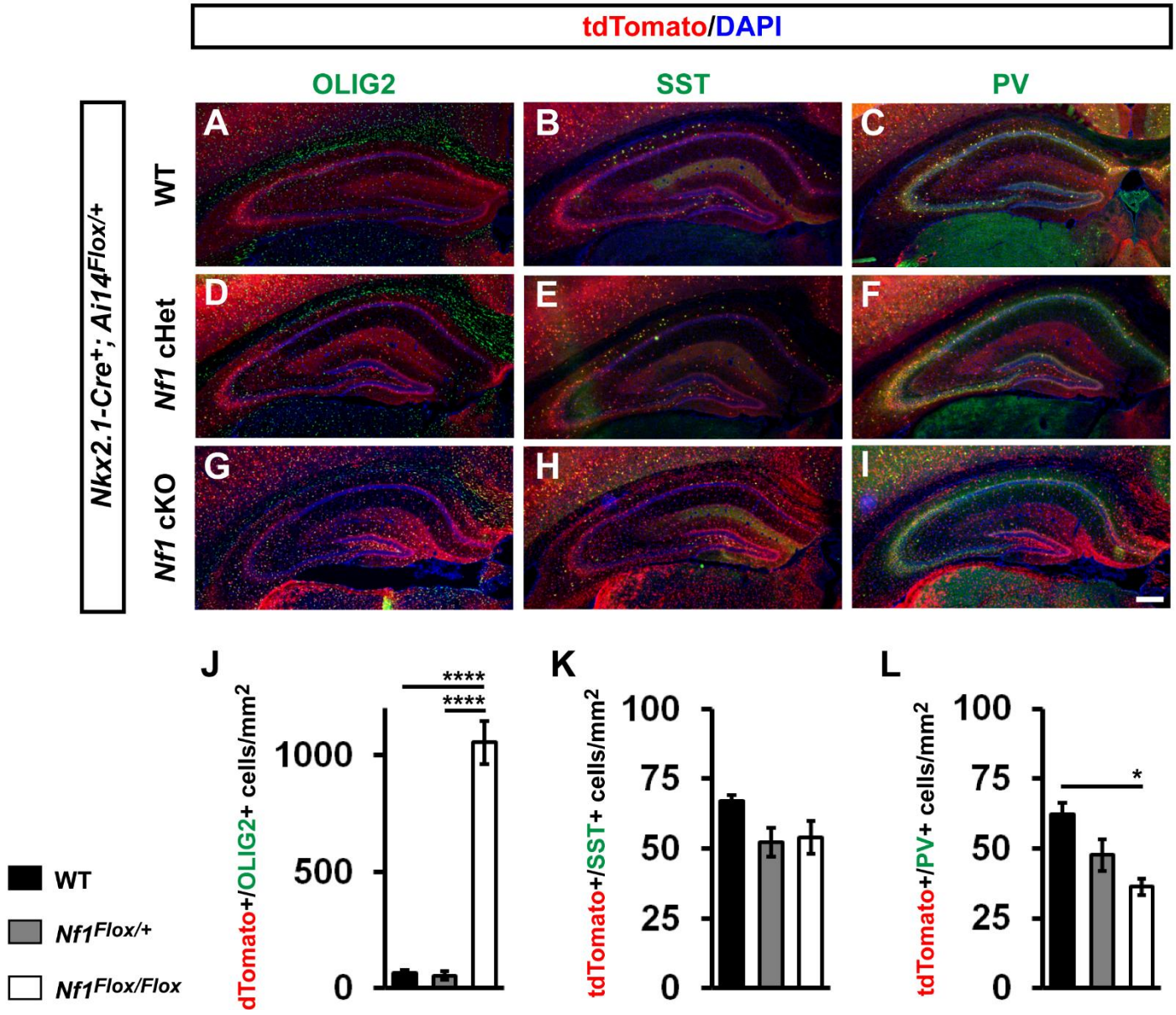

Supplemental Figure 4: *Nkx2.1-Cre* conditional loss of *Nf1* leads to an increase in immature oligodendrocytes and a loss of PV+ CINs in the hippocampus.

P30 WT (**A-C**), *Nf1* cHet (**D-F**) and *Nf1* cKO (**G-I**) coronal tissue was visualized for tdTomato (*Nkx2.1-Cre*-lineages) and either Olig2, SST or PV. (**J**) Quantification of co-labeled tdTomato/OLIG2+ cell density. (**K**) Quantification of co-labeled tdTomato/SST+ cell density. (**L**) Quantification of co-labeled tdTomato/PV+ cell density. Data are expressed as the mean ± SEM. All groups, n = 3. * $p < 0.05$, **** $p < 0.0001$. Scale bar in (**I**) = 100 µm.

Supplemental Figure 5

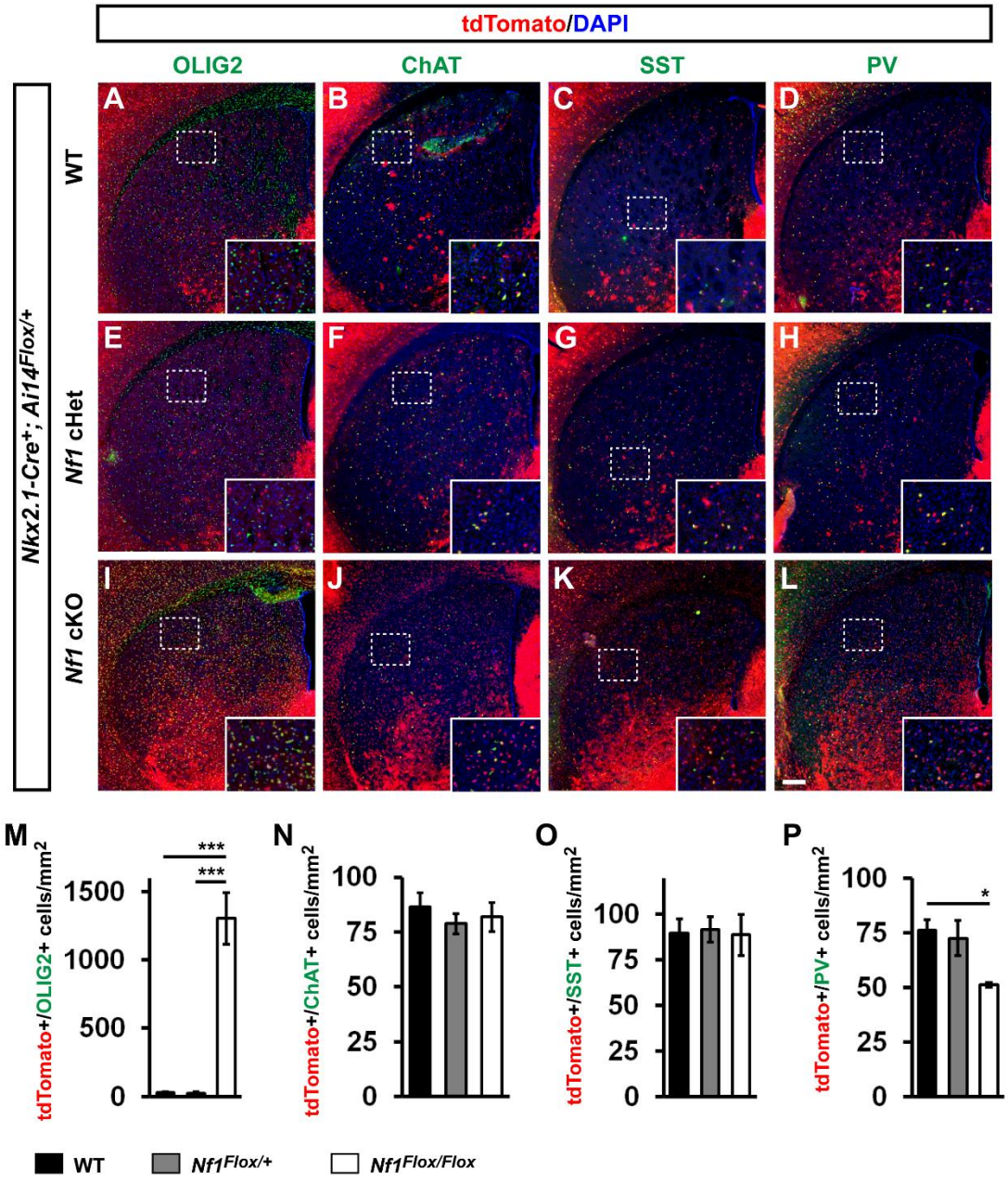

Supplemental Figure 5: *Nkx2.1-Cre* conditional loss of *Nf1* leads to an increase in immature oligodendrocytes and a loss of PV+ CINs in the striatum.

P30 WT, *Nf1* cHet and *Nf1* cKO coronal tissue was visualized for tdTomato (*Nkx2.1-Cre*-lineages) and either Olig2 (**A, E, I**), ChAT (**B, F, J**), SST (**C, G, K**) or PV (**D, H, L**). Cell density quantification of tdTomoto+ cells co-labeled for Olig2+ (**M**), ChAT (**N**), SST (**O**) and PV (**P**). Quantification of co-localized tdTomato/SST+ cell density did not reveal differences between genotypes (**E**). All data are expressed as the mean ± SEM. WT, n = 4, cHet, n = 3 and cKO, n = 3. * $p < 0.05$, **** $p < 0.0001$. Scale bar in **L** = 100 µm.

Supplemental Figure 6

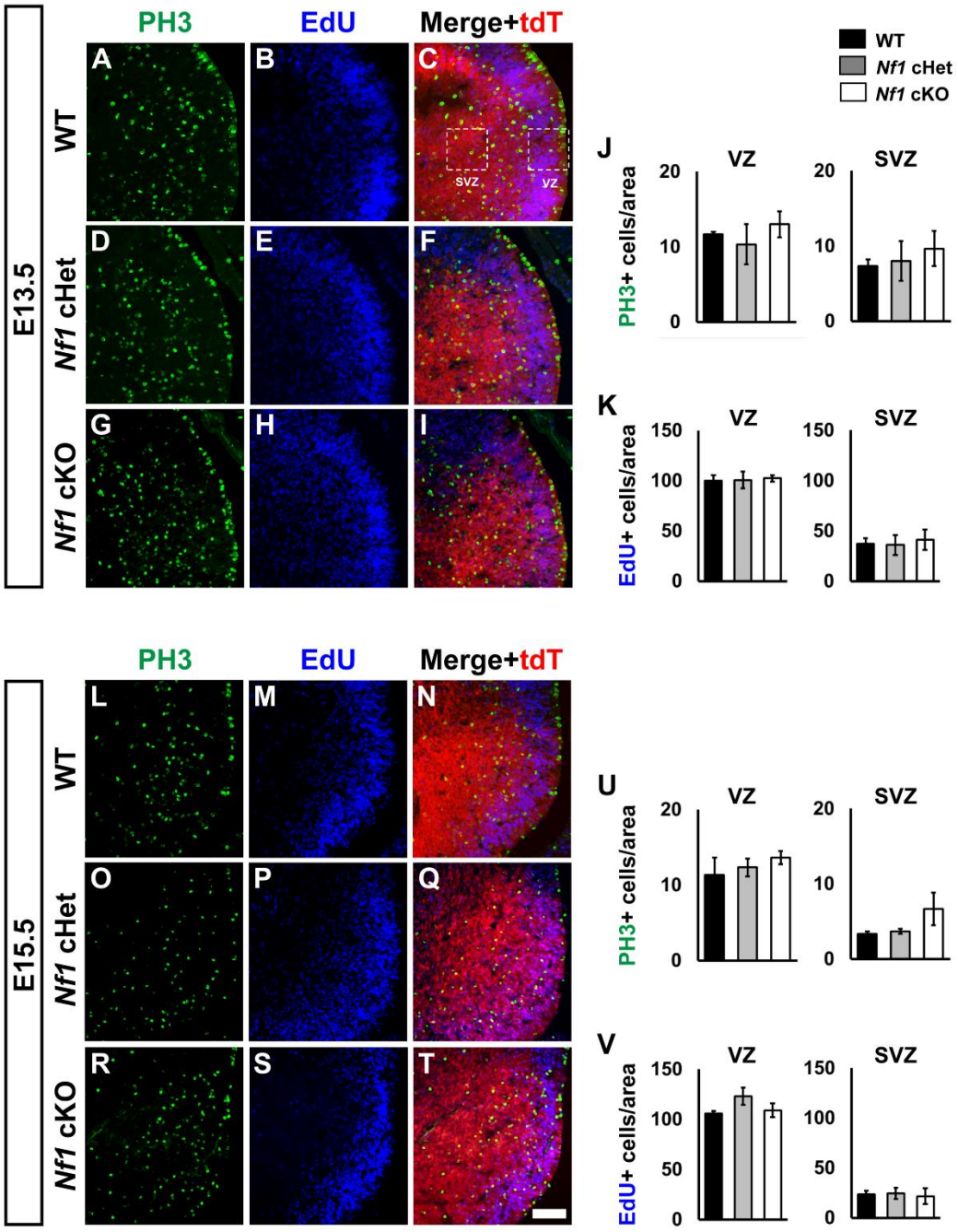

Supplemental Figure 6: Normal proliferation in the MGE of *Nf1* mutants.

E13.5 WT (**A-C**), *Nf1* cHet (**D-F**) or *Nf1* cKO (**G-I**) coronal brain sections were co-labeled for PH3, EdU and tdTomato (tdT). Inset boxes in (**C**) denote the ventricular zone (VZ) and sub ventricular zone (SVZ) regions that cells were counted from. Quantification of the cell density of either PH3+ cells (**J**) or EdU+ cells (**K**) in both the VZ and SVZ at E13.5. E15.5 WT (**L-N**), *Nf1* cHet (**O-Q**) or *Nf1* cKO (**R-T**) sections co-labeled for PH3, EdU and tdTomato (tdT). Quantification of the cell density of either PH3+ cells (**U**) or EdU+ cells (**V**) in both the VZ and SVZ at E15.5. Data are expressed as the mean ± SEM. n = 3, all groups. Scale bar in (**T**) = 100 µm.

Supplemental Figure 7

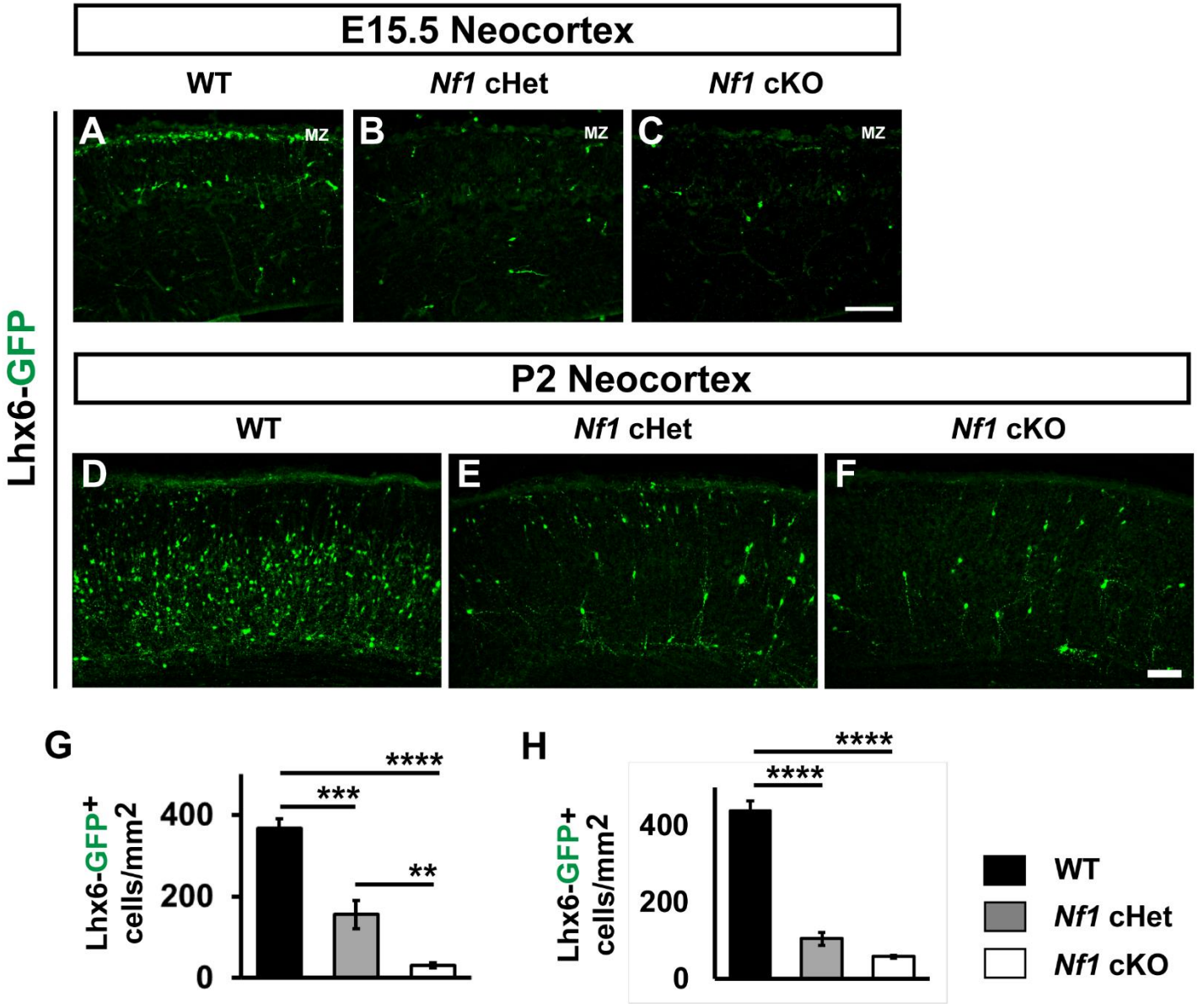

Supplemental Figure 7: A *Lhx6-GFP* reporter shows reduced expression in cHets and cKOs.

E15.5 WT, cHet and cKO neocortices were probed for *Lhx6-GFP* expression (**A-C**). (MZ) denotes the marginal zone. P2 brains from the same genotypes were visualized for *Lhx6-GFP* expression (**D-F**). Quantification of *Lhx6-GFP* expressing CINs in the E15.5 neocortex (**G**). or in the P2 neocortex (**H**). Data are expressed as the mean ± SEM. n = 3, all groups. ** $p < 0.01$; *** $p < 0.001$; **** $p < 0.0001$. Scale bars in (**C, D**) = 100 µm.

Supplemental Figure 8

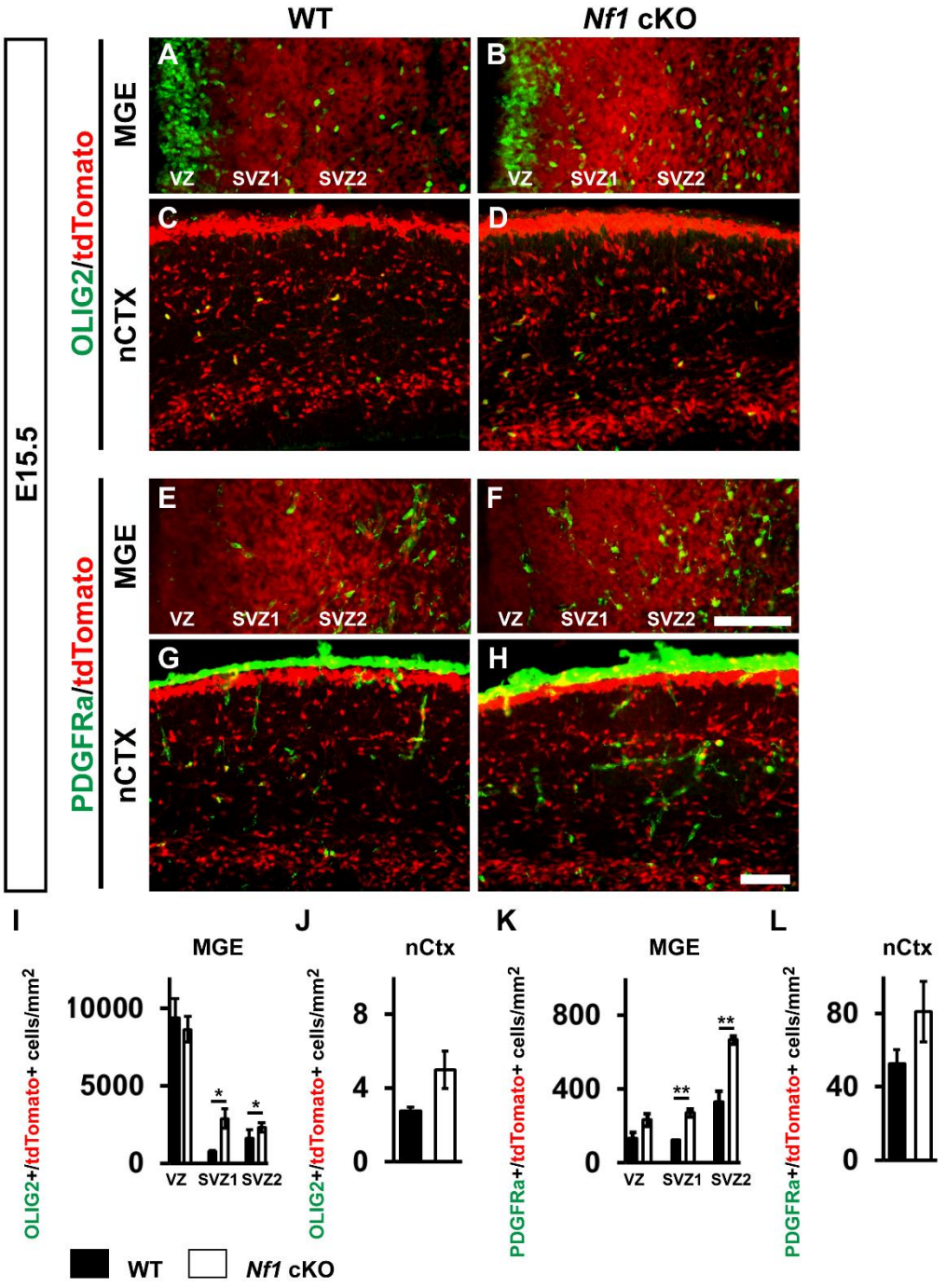

Supplemental Figure 8: Increased OLIG2+ and PDGFRa+ cells in embryonic cKO brains.

E15.5 WTs and cKOs were probed for OLIG2 expression in the MGE (**A, B**) and the neocortex (nCtx) (**C, D**). TdTomato expression labels *Nkx2.1-Cre*-lineages. The same tissues were also labeled for PDGFRa (**E-H**). Quantification of OLIG2+ cells in the MGE (**I**) and nCtx (**J**) or PDGFRa+ cells in the MGE (**K**) and nCtx (**L**). Data are expressed as the mean ± SEM. n = 4, OLIG2 counts, n = 3, PDGFRa counts. * $p < 0.05$; ** $p < 0.01$. Scale bars in (**F, H**) = 100 µm.

Supplemental Figure 9

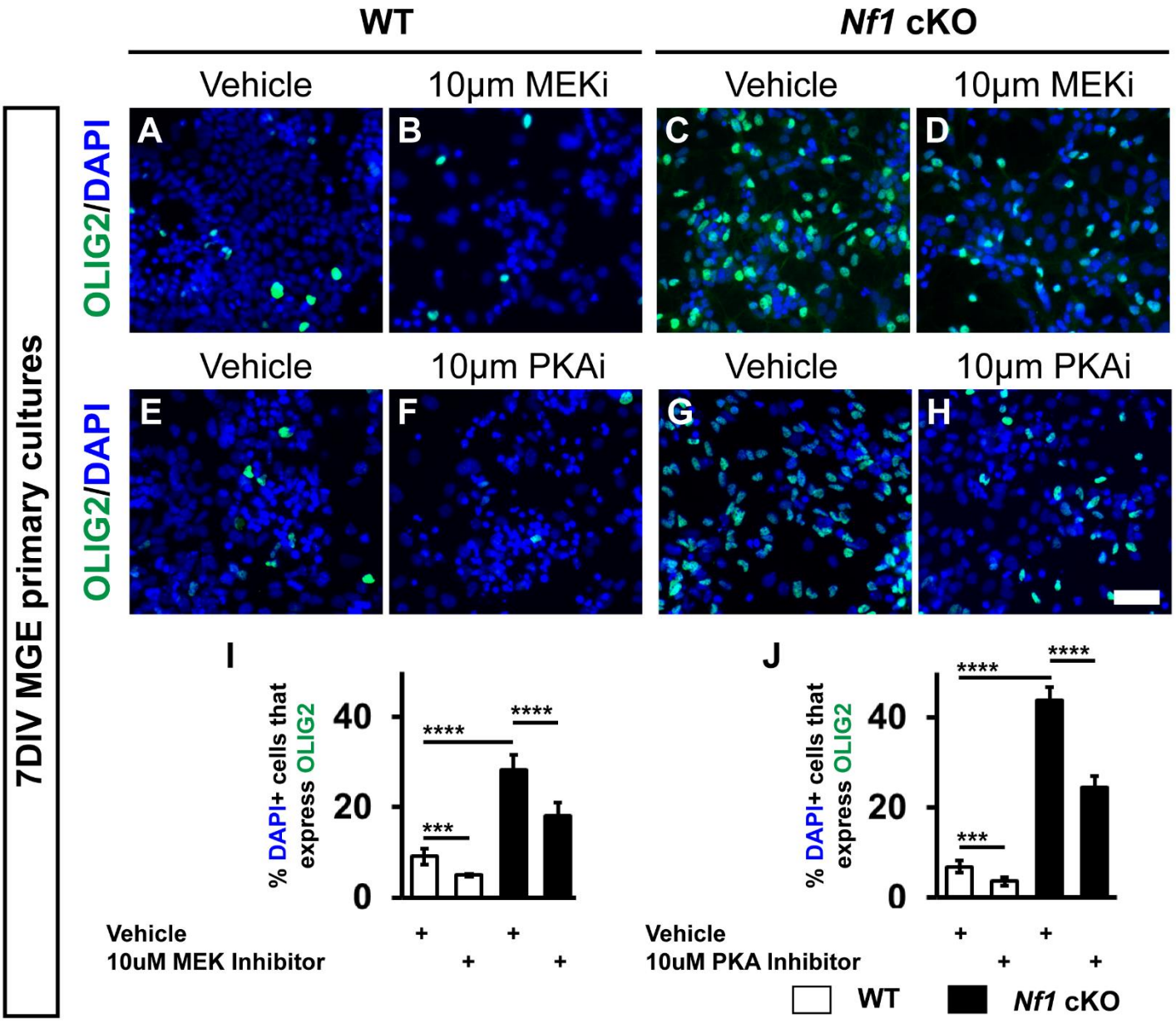

Supplemental Figure 9: Partial rescue of OLIG2 expression with SL327 or H-89.

E13.5 WT or cKO MGE cells were cultured for seven days in the presence of either vehicle, SL327 or H-89 and then assessed for OLIG2 expression (**A-H**). Quantification of OLIG2+ cells normalized to DAPI numbers with MEK inhibition (SL327, MEKi) (**I**) or PKA inhibition (H-89, PKAi) (**J**). Data are expressed as the mean ± SEM. n = 4, all groups. *** $p < 0.001$; **** $p < 0.0001$. Scale bar in (**H**) = 100 μm.

Supplemental references

1. L. Madisen, *et al.*, A robust and high-throughput Cre reporting and characterization system for the whole mouse brain. *Nat. Neurosci.* **13**, 133–140 (2010).

2. Y. Zhu, *et al.*, Ablation of NF1 function in neurons induces abnormal development of cerebral cortex and reactive gliosis in the brain. *Genes Dev.* **15**, 859–876 (2001).

3. Q. Xu, M. Tam, S. A. Anderson, Fate mapping Nkx2.1-lineage cells in the mouse telencephalon. *J. Comp. Neurol.* **506**, 16–29 (2008).

4. S. Hippenmeyer, *et al.*, A developmental switch in the response of DRG neurons to ETS transcription factor signaling. *PLoS Biol.* **3**, e159 (2005).

5. D. Vogt, K. K. A. Cho, A. T. Lee, V. S. Sohal, J. L. R. Rubenstein. The parvalbumin/somatostatin ratio is increased in Pten mutant mice and by human PTEN ASD alleles. *Cell Rep.* **11**, 944–956 (2015).

6. X. Duan, *et al.*, Cadherin Combinations Recruit Dendrites of Distinct Retinal Neurons to a Shared Interneuronal Scaffold. *Neuron* **99**, 1145-1154.e6 (2018).

7. A. Paul, *et al.*, Transcriptional Architecture of Synaptic Communication Delineates GABAergic Neuron Identity. *Cell* **171**, 522-539.e20 (2017).